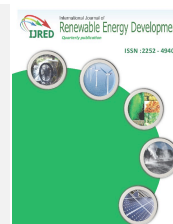




Contents list available at IJRED website

Int. Journal of Renewable Energy Development (IJRED)

Journal homepage: <http://ejournal.undip.ac.id/index.php/ijred>



Research Article

Biofuels Production from Catalytic Cracking of Palm Oil Using Modified HY Zeolite Catalysts over A Continuous Fixed Bed Catalytic Reactor

I. Istadi*, Teguh Riyanto, Luqman Buchori, Didi D. Anggoro, Andre W.S. Pakpahan, Agnes J. Pakpahan

Department of Chemical Engineering, Faculty of Engineering, Universitas Diponegoro, Semarang, Central Java, 50275, Indonesia

ABSTRACT. The increase in energy demand led to the challenging of alternative fuel development. Biofuels from palm oil through catalytic cracking appear as a promising alternative fuel. In this study, biofuel was produced from palm oil through catalytic cracking using the modified HY zeolite catalysts. The Ni and Co metals were impregnated on the HY catalyst through the wet-impregnation method. The catalysts were characterized using X-ray fluorescence, X-ray diffraction, Brunauer–Emmett–Teller (BET), Pyridine-probed Fourier-transform infrared (FTIR) spectroscopy, and Scanning Electron Microscopy (SEM) methods. The biofuels product obtained was analyzed using a gas chromatography-mass spectrometry (GC-MS) method to determine its composition. The metal impregnation on the HY catalyst could modify the acid site composition (Lewis and Brønsted acid sites), which had significant roles in the palm oil cracking to biofuels. Ni impregnation on HY zeolite led to the high cracking activity, while the Co impregnation led to the high deoxygenation activity. Interestingly, the co-impregnation of Ni and Co on HY catalyst could increase the catalyst activity in cracking and deoxygenation reactions. The yield of biofuels could be increased from 37.32% to 40.00% by using the modified HY catalyst. Furthermore, the selectivity of gasoline could be achieved up to 11.79%. The Ni and Co metals impregnation on HY zeolite has a promising result on both the cracking and deoxygenation process of palm oil to biofuels due to the role of each metal. This finding is valuable for further catalyst development, especially on bifunctional catalyst development for palm oil conversion to biofuels.

Keywords: biofuels; palm oil; catalytic cracking; deoxygenation; Ni-Co/HY; HY Zeolite

Article History: Received: 2nd October 2020; Revised: 2nd November 2020 ; Accepted: 6th November 2020; Available online: 12th Nov 2020

How to Cite This Article: Istadi, I., Riyanto, T., Buchori, L., Anggoro, D.D., Pakpahan, A.W.S. and Pakpahan, A.J. (2021) Biofuels Production from Catalytic Cracking of Palm Oil Using Modified HY-Zeolite Catalysts over A Continuous Fixed Bed Catalytic Reactor. *International Journal of Renewable Energy Development*, 10(1), 149-156.

<https://doi.org/10.14710/ijred.2021.33281>

1. Introduction

Due to the high demand for energy and a decrease in fossil fuel resources, the development of biofuels to support the energy demand has increased. Several processes have been developed in order to produce high-quality biofuels, including transesterification and cracking processes (Riyanto *et al.* 2020; Buchori *et al.* 2016). The transesterification process only produces diesel range biofuel, which is generally called biodiesel. However, biodiesel has high hygroscopicity that could cause clogging in the engine filter, and before it is used, it has to be mixed with fossil fuels (Sousa *et al.* 2018). The other processes are cracking processes, including pyrolysis/thermal cracking, catalytic cracking, and hydrocracking (Riyanto *et al.* 2020). However, the catalytic cracking is a promising process due to low energy consumption, high product diversity, and clean product produced (Bhatia *et al.* 2009; Demirbas 2009; Istadi *et al.* 2019; Riyanto *et al.* 2020). Therefore, it is necessary to explore the catalytic cracking process for biofuel production.

The most favorable feedstock on biofuel production through catalytic cracking is vegetable oil, especially palm oil, due to its high content in long-chain hydrocarbon (Bhatia *et al.* 2009). On the other hand, palm oil is abundantly available in the world, especially in Indonesia and Malaysia. The biofuels produced through catalytic cracking of vegetable oil have no pollutants, such as: sulfur, nitrogen, and heavy metals (Ramya *et al.* 2012). Consequently, the combustion process of these biofuels produces better emissions than the combustion process of fossil fuels.

The development in the catalytic cracking process of palm oil into biofuel is focused on the development of the suitable catalysts used. The characteristic of the catalysts used has a significant role in biofuel production through the palm oil cracking process, especially the acidity of the catalysts. It was reported that the acidity of the catalysts affected the biofuel product distributions (Istadi *et al.* 2020). The Lewis acid sites promoted the formation of short-chain hydrocarbons fraction, while the Brønsted acid sites promoted the formation of long-chain

* Corresponding author: istadi@che.undip.ac.id

hydrocarbons fraction. Istadi *et al.* (2020) reported that the Lewis acid sites on acid-modified Residue Fluid Catalytic Cracking (RFCC) catalysts waste lead to the formation of short-chain hydrocarbons fraction, which was represented as gasoline fraction. Based on this understanding, it is necessary to develop the catalysts with high Lewis acid sites in order to increase the production of short-chain hydrocarbons fraction. However, the Lewis acid sites lead to coke formation caused by the deactivation process of the catalysts (Xu *et al.* 2012; Feng *et al.* 2014; Istadi *et al.* 2020). Therefore, the appropriate amount of Lewis acid sites on the catalysts for the palm oil cracking process needs to be explored.

Mostly, higher Lewis acid site catalysts were developed through metal transition impregnation due to the presence of unoccupied orbitals that can still accept electrons (Sugiarti *et al.* 2020; Anggoro *et al.* 2017). Sriatun *et al.* (2019) reported that Nickel (Ni) metal impregnation on ZSM-5 catalyst could increase the Lewis acid site on the catalyst. On the other hand, Roesyadi *et al.* (2013) also reported that introducing Ni metal to the HZSM5 catalyst could increase the gasoline selectivity on palm oil cracking. Therefore, it is necessary to develop a catalyst with Ni as the active site for the palm oil cracking process to produce biofuels. However, the individual metallic Ni only led to the C–H bonds cleavage (Li *et al.* 2019). Based on this understanding, it is expected that the biofuels product produced by Ni-based catalysts will still have a high oxygenated compound. The oxygenated compound in the biofuels should be limited. A high amount of oxygenated components in biofuels leads to a low heating value chemicals.

On the other hand, Cobalt (Co) has been widely used for deoxygenation reaction (Sriifa *et al.* 2015; Ranga *et al.* 2019). Co has high activity and high selectivity to promote deoxygenation reaction (Ranga *et al.* 2019). Based on those understandings, the Ni and Co metals are used to develop high activity catalysts for biofuels production from the palm oil cracking process. Ni and Co are impregnated on HY catalyst. However, the study of HY zeolite modification through impregnation of Ni and Co metals in order to increase the activity of the catalysts on palm oil cracking to biofuels is limited. Furthermore, the effect of each metal on the catalyst properties and catalyst activity in biofuels production from palm oil cracking are studied in this study. In addition, the effect of mixed metal impregnation is also studied. The impregnation of both metals is expected to increase the activity of the catalysts on both palm oil cracking and deoxygenation.

2. Materials and Methods

2.1 Materials

The HY zeolite obtained from Zeolyst International was used as a catalyst. The metal precursors used for the modification of the catalysts were Nickel (II) nitrate hexahydrate ($\text{Ni}(\text{NO}_3)_2 \cdot 6\text{H}_2\text{O}$) (Merck, 99%), and Cobalt (II) nitrate hexahydrate ($\text{Co}(\text{NO}_3)_2 \cdot 6\text{H}_2\text{O}$) (Merck, 99%). In order to investigate the activity of the catalysts on the cracking process, the commercial refined palm oil from the local market was used as the feedstock. The composition of the feedstock is provided in Table 1. The highest components present are palmitic acid and oleic acid.

Table 1

Composition of palm oil feedstock

Component	Composition (%)
Palmitic acid (C16:0)	44.53
Stearic acid (C18:0)	1.80
Oleic acid (C18:1)	41.91
1-Tridecene	5.32
2,6,10,14,18-Penta Methyl Eicosa Pentane	6.44
Total	100.00

Palmitic acid is a saturated fatty acid, while oleic acid is an unsaturated fatty acid. The nitrogen (N_2) (UHP, 99.9%) gas was used for flushing the oxygen in the experimental rig before the cracking process was conducted.

2.2 Catalysts Preparation

The HY zeolite was dried at 110 °C for 12 h in an electric oven (Memmert) and calcined for 4 h at 500 °C in a box furnace (NEY FULCAN 3-550). This obtained catalyst was denoted as HY catalyst. The Co and Mo metals were impregnated on the HY zeolite using the wet impregnation method. The impregnation of metals was designed to impregnate 1% of metal on HY Zeolite. Before the impregnation process, HY zeolite was dried in an electric oven (Memmert) at 110 °C for 12 h. The metal precursor solution for impregnation was prepared using demineralized water and metal precursors. A certain amount of metal precursor was dissolved in 250 mL of demineralized water so that the metal content of the synthesized catalyst was 1% for single metal impregnation. For the co-impregnation process of Ni and Co metals on HY zeolite, both metal precursors (Ni and Co) with a mass ratio of 1:1 were dissolved in 250 mL of demineralized water so that the metal content of the synthesized catalyst was 0.5% of each metal (total metal content of 1%). After the drying process, the dried HY zeolite was soaked in the metal precursor solution at room temperature for 30 min with mild stirring. The suspended solid from this process was then filtered and washed using demineralized water until neutral. Hereafter, this solid was dried at 110 °C for 12 h and calcined at 500 °C for 4 h. The calcination is conducted to remove the nitrate molecule and to adjust the surface properties and phase structure of catalysts as reported elsewhere (Kamal *et al.* 2020). The catalyst impregnated with Ni denoted Ni/HY catalyst, Co/HY for Co impregnation, and Ni-Co/HY for co-impregnation of Ni and Co. The obtained catalysts were pelleted and crushed into 1 – 1.18 mm.

2.3 Catalysts Characterization

The synthesized catalysts were characterized using several methods. The metal composition in the catalysts was determined using X-ray Fluorescence (XRF) (Rigaku Supermini 200 Benchtop WDXRF Spectrometer) method. In order to determine the crystal structure of the catalysts, the synthesized catalysts were characterized using X-ray Diffraction (XRD) (Shimadzu 7000) method. The diffraction patterns were generated at 2 θ angle ranges of 10–60° with a scanning speed of 5° min⁻¹ which Cu-K α

radiation ($\lambda = 1.54 \text{ \AA}$) was operated at 30 mA and 30 kV. Brunauer–Emmett–Teller (BET) surface area method was used to determine the surface area of the catalysts (ChemBET PULSAR Quantachrome) after being degassed at 300 °C for 5 h. Furthermore, the acid site amount and acid site type were determined using Pyridine-probed Fourier-transform infrared (FTIR) spectroscopy method. The FTIR spectra were monitored at a wavenumber of 1600 – 1400 cm^{-1} . The adsorption band appeared at 1455 cm^{-1} represents the Lewis acid site, while the absorption band appeared at around 1545 cm^{-1} represents the Brønsted acid site (Istadi *et al.* 2020; Vieira *et al.* 2015). The amount of Brønsted and Lewis acid sites on the catalyst is expressed as the number of pyridines adsorbed at each acid site per mass of catalyst. The acid site amount was calculated related to the integrated absorbances of each peak representing Lewis and Brønsted acid sites (Bailleul *et al.* 2019). The surface morphology of the catalysts was investigated using Scanning Electron Microscopy (SEM) method.

2.4 Cracking Process

The activity of the catalysts was evaluated through the cracking process of palm oil over a continuous fixed bed catalytic reactor. The experimental rig for cracking reaction is provided in Fig. 1. The reactor used is a stainless-steel reactor with an inside diameter of 2.54 cm and a reactor length of 30 cm. The catalysts (5 g) were put inside the reactor which was supported using glass wool as displayed in Fig. 1. Before the reaction, the rig was flushed using nitrogen gas, flowed at 0.1 NL/min for 30 min to eliminate the oxygen trapped in the rig. The palm oil feedstock was fed to the reactor using a peristaltic pump at a certain flow rate so that the weight hourly space velocity (WHSV) was 0.365 min^{-1} . Several researchers reported that the cracking process of vegetable oil was conducted in a reactor temperature range of 340–500 °C, and the most cracking process was conducted at ~450 °C (Chew and Bhatia 2008; Riyanto *et al.* 2020).

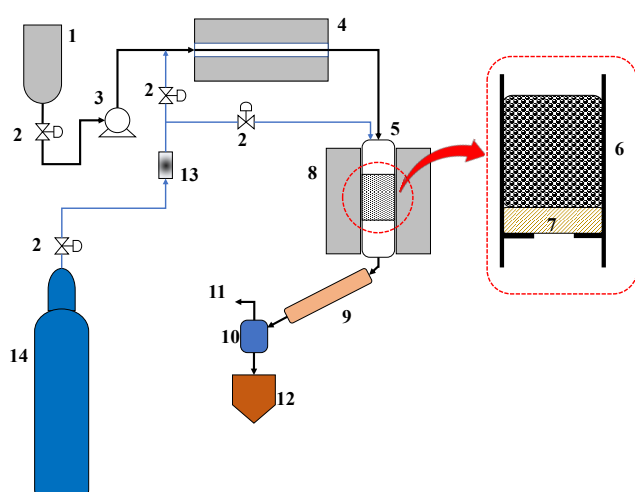


Fig. 1 Scheme of the experimental set up: (1) Palm oil feedstock tank, (2) Gate valve, (3) Peristaltic pump, (4) Preheater, (5) Reactor tube, (6) Catalysts packing, (7) Glass wool, (8) Electric heating furnace as reactor heater, (9) Condensor, (10) Gas-liquid separator, (11) Gas by product, (12) Liquid fuels product, (13) Gas flowmeter, and (14) Nitrogen gas tank.

Therefore, in this study, the cracking reaction was conducted at a temperature of 450 °C. The cracking product was condensed through the condenser and separated with the uncondensed by-product. The liquid fuel products were then collected in a flask for further analysis as a raw biofuels product called organic liquid product (OLP). The raw biofuels product was collected during the first 2 h (the basis of performance calculation) after a steady state was achieved (30 min after the reaction was started). The collected liquid fuels/OLP as a raw product were then analyzed using gas chromatography-mass spectrometry (GC–MS) MS (QP2010S SHIMADZU, DB-1 column) to determine the composition of the components. The samples were analyzed at 50 °C oven temperature (held for 5 min) and ramped 10 °C/min to 260 °C and held for 33 min.

In order to evaluate the performance of the catalytic hydrocracking process, some parameters, such as palm oil conversion, biofuels product yield, and selectivity, were used. The palm oil conversion (X), the yield of OLP, gas, and coke (Y_i), and selectivity of the mixed gasoline, kerosene, and diesel fraction (S_j) were calculated using the following equations:

$$X (\%) = \frac{m_{feed} - m_{unreacted\ feed}}{m_{feed}} \times 100 \quad (1)$$

$$Y_i (\%) = \frac{m_i}{m_{feed}} \times 100 \quad (2)$$

$$S_j (\%) = \frac{m_j}{m_{feed} - m_{unreacted\ feed}} \times 100 \quad (3)$$

where, m_{feed} is the mass of palm oil-fed, $m_{unreacted\ feed}$ is the mass of unreacted palm oil, m_i is the mass of component i (in OLP, gas, and coke phases), and m_j represents the mass of component j (mixed gasoline, kerosene, and diesel). The gasoline, kerosene, and diesel fraction were categorized based on carbon ranges of hydrocarbons from the GC–MS analysis results as reported elsewhere (Istadi *et al.* 2020), where $C_5 - C_{12}$ ranges were categorized as a gasoline fraction, $C_{13} - C_{14}$ ranges were categorized as a kerosene fraction, and $C_{15} - C_{18}$ ranges were categorized as diesel fraction (Istadi *et al.* 2020).

3. Results and Discussions

3.1 Catalysts Characterization

3.1.1 X-Ray Fluorescence (XRF) Analysis

XRF analysis was introduced in order to determine the metal content that was impregnated on the HY catalyst. As can be seen in Table 2, the Ni and Co metals are successfully impregnated on the HY catalyst. However, the amount of metal that was impregnated on the HY catalyst is lower than the design. As designed, the Ni and Co content should be 1% at single metal impregnation and 0.5% for each metal at double metal impregnation. The difference in the amount of metal between the design and the obtained is due to the low efficiency of the impregnation process. It is suggested that the metal is not completely impregnated on the HY catalyst. On the other

hand, this tendency is also due to the losses during the washing step. Several amounts of the impregnated metal were washed during the washing process. This finding is in agreement with the finding of Mhadmhan *et al.* (2018). They reported that the Ni metal could be washed by water during the filtration/washing step. It is due to the low interaction between the metal and HY catalyst.

3.1.2 X-Ray Diffraction (XRD) Analysis

XRD analysis was used to determine the crystal structure of the catalysts that have been synthesized. The XRD pattern of the synthesized catalysts is provided in Fig. 2. As can be observed from Fig. 2, the XRD pattern of the HY catalyst after metal impregnation is not changed. It is indicated that the crystal structure of the catalyst is not changed significantly after the metal impregnation. Therefore, it is suggested that the impregnation of Ni and Co on HY catalysts does not change the crystallinity of the catalysts. In addition, the peak corresponds to the Ni and/or Co metal does not appear in the synthesized catalysts. This tendency is due to the low amount of metal impregnated on the catalysts. Based on XRF analysis results (Table 2), the metal amount impregnated on the catalysts is lower than 1%. On the other hand, the absence of Ni and/or Co peak in the XRD pattern of the catalysts is caused by the dispersion of the metals on the catalysts (Anggoro *et al.* 2017). Therefore, it is suggested that the Ni and Co metals are highly dispersed on the catalyst.

3.1.3 Brunauer–Emmett–Teller (BET) Analysis

BET analysis was used to determine the surface area of the catalysts. The impregnation of metal is expected to increase the surface area of the catalysts through the decoration of the supported catalyst by metal (Mhadmhan *et al.* 2018). However, it can be seen in Table 2 that the surface area of the catalysts decreases after the metal impregnation. This tendency is affected by the pore blocking caused by metal. The presence of metal on the HY zeolite may block the pore mouth. On the other hand, the metal can also be impregnated on the pore channels that affected the decrease in the surface area. It is true since the HY catalyst is a porous material. The impregnation of metal on the porous material can decrease the surface area due to the pore blocking process (Istadi *et al.* 2019; Adeoye *et al.* 2017). Therefore, it is suggested that the

decrease in the HY catalysts surface area after Ni and Co impregnation is due to the pore blocking by the metals.

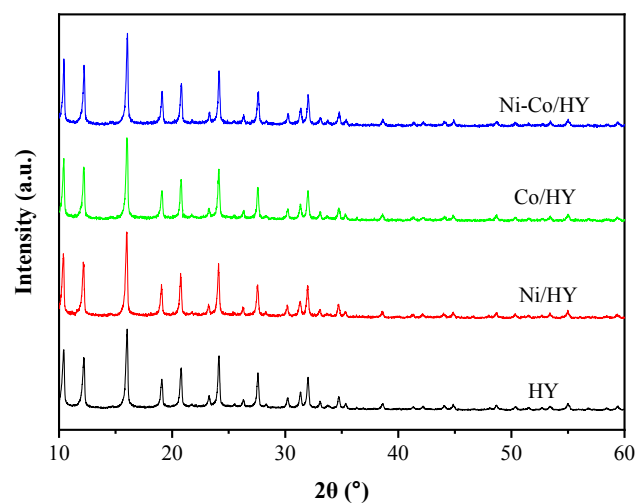


Fig. 2 XRD pattern of the catalysts

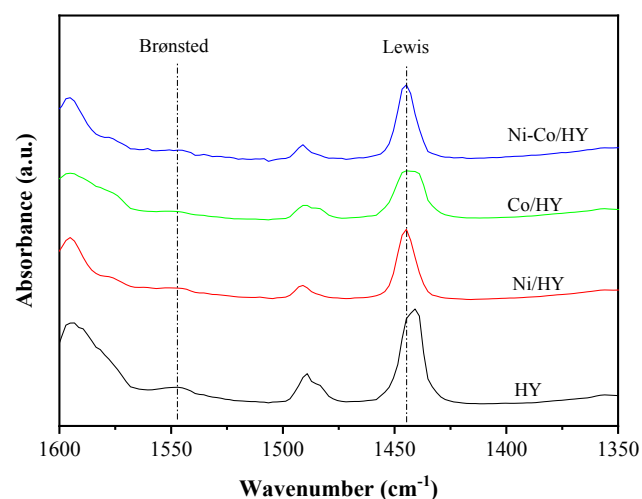


Fig. 3 Pyridine-probed Fourier-Transform Infrared Spectroscopy (Py-FTIR) of the catalysts

Table 2
Physico-chemical properties of the catalysts

Catalysts	Metal content (%)		Surface area (m ² /g)	Acid site amount (μmol/g)			L/B ratio*
	Ni	Co		Lewis	Brønsted	Total	
HY	-	-	633.639	56.364	1.642	58.006	34.326
Ni/HY	0.367	-	547.532	58.648	1.551	60.199	37.813
Co/HY	-	0.475	565.945	23.880	2.595	26.475	9.202
Ni-Co/HY	0.304	0.295	563.596	51.128	1.136	52.264	45.007

*ratio of Lewis to Brønsted acids site

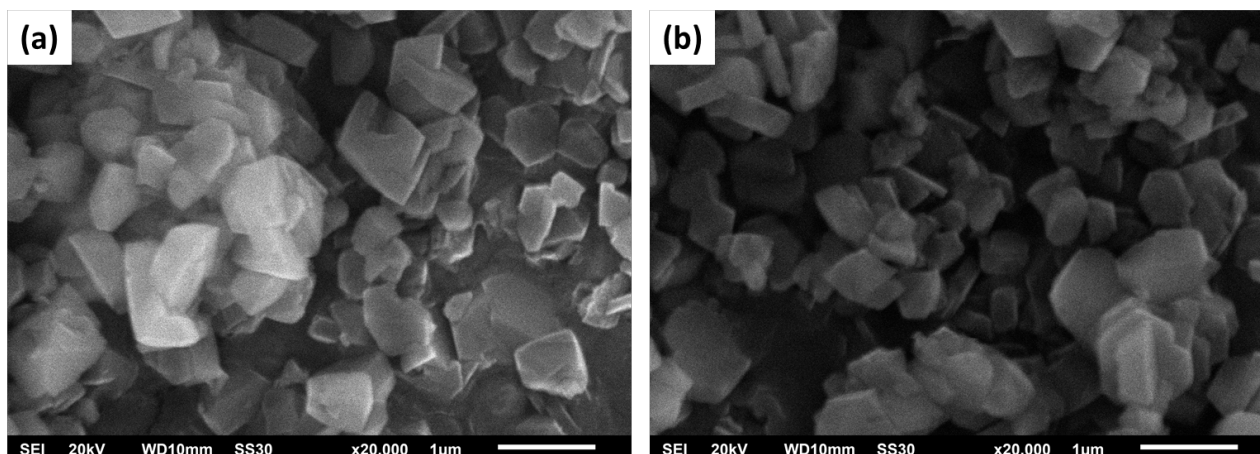


Fig. 4 Surface morphology of (a) HY and (b) Ni-Co/HY catalysts

3.1.4 Pyridine-probed Fourier-Transform Infrared Spectroscopy (Py-FTIR) Analysis

The Py-FTIR analysis was used to determine the acid site amount on the catalysts. In addition, the Py-FTIR analysis was also used to determine the acid site type presence on the catalysts. Pyridine used as the probe molecule can interact with the acid sites presence on the catalysts. Pyridine binds coordinatively with the Lewis acid site and binds with the Brønsted acid site to form pyridinium ion. These interactions were then detected by using FTIR. The adsorption band of the Lewis acid site will appear at around 1455 cm^{-1} , while the absorption band of the Brønsted acid site will appear at around 1545 cm^{-1} (Istadi *et al.* 2020; Vieira *et al.* 2015). The infrared spectroscopy patterns of the catalysts are presented in Fig. 3, and the calculated acid site amount is provided in Table 2.

As can be observed, the acid site amount of the catalysts is affected by the metal impregnation process. The highest acid site amount is Ni/HY catalyst. The impregnation of Ni on the HY catalyst increase the Lewis acid site amount and decrease the Brønsted acid site amount. The increase of the Lewis acid site after Ni impregnation is expected by the fact that the Ni metal can act as the Lewis acid site, as reported by Sriatun *et al.* (2019). On the other hand, it is found that the impregnation of Co metal on HY zeolite decreases the acid site amount. However, the co-impregnation of Ni and Co on HY could increase the ratio of Lewis to Brønsted acid site (L/B ratio) on the catalyst (Table 2). Therefore, it is suggested that the co-impregnation of Ni and Co on HY decreases the total acid site amount of HY catalyst; however, this co-impregnation leads to an increase of L/B ratio. The L/B ratio is an important parameter since the composition of Lewis and Brønsted acid sites on the catalysts has a significant role in the cracking process, as reported by several researchers (Rogers and Zheng 2016; Hewer *et al.* 2018; Istadi *et al.* 2020). It was reported that the component distribution of the product from palm oil cracking depended mainly on the distribution of Lewis and Brønsted acid sites (L/B ratio) (Istadi *et al.* 2020). Therefore, L/B ratio has to be considered in the catalyst development for the cracking process.

3.1.5 Scanning Electron Microscopy (SEM) Analysis

SEM analysis was conducted to investigate the surface morphology of the catalysts. Fig. 4 shows the surface morphology of HY and Ni-Co/HY catalysts. As can be seen in Fig. 4, the surface morphology of HY catalyst after Ni-Co impregnation does not change. On the other hand, the particle size of the catalysts also seems not changed. This fact confirms that the impregnation of Ni and Co on the HY catalyst does not change the surface morphology of the catalyst. Furthermore, it is suggested that the Ni and Co metal are highly dispersed on the HY catalyst. It is in accordance with the result of XRD analysis (section 3.1.2), which is indicated through the un-appeared peaks correspond to Ni and Co metal.

3.2 Catalysts Performance on the Palm Oil Cracking

The performance of the catalysts is observed on the cracking reaction of palm oil to produce biofuels. The cracking reaction was conducted at a fixed-bed catalytic reactor. The result of the catalytic cracking process of palm oil is provided in Table 3. As can be observed, the conversion values obtained by all catalysts are relatively unchanged. On the other hand, the obtained conversion value is close to 100%. It means that all catalysts have high activity on the palm oil cracking process. This high performance/activity is affected by the acid site amount and the surface area of the catalysts. It is true since the formation of the carbocations initiates the catalytic cracking reaction. These carbocations are formed over acid catalysts. The mechanism of the formation of the carbocations can be found elsewhere (Corma and Orchillés 2000). The carbocations are formed through the protonation of reactant molecules by the Brønsted acid site and/or by the hydrogen abstraction of reactant molecules by the Lewis acid site (Corma and Orchillés 2000). However, since the acid site amounts of the catalysts are different, it is expected that there is another catalyst characteristic that may affect the activity of the catalysts. As reported by several researchers, it is found that the surface area of the catalysts has also affected the performance of the catalysts (Istadi *et al.* 2019; Yigezu and Muthukumar 2014). Catalysts with a large surface area can reduce the mass transfer limitation; therefore, the reaction can be accelerated. Hence, it is suggested that the

high conversion value obtained is due to the high catalysts surface area and due to the presence of both Brønsted and Lewis acid sites on the catalysts.

As can be seen in Table 3, the highest yield of OLP, as well as the yield of coke, are obtained by Ni/HY catalyst. Based on Py-FTIR analysis, the Ni/HY catalyst has the highest acid site amount. Therefore, it is suggested that the high yield of OLP obtained is affected by the highest acid site amount on Ni/HY catalyst. It is true since the acid sites on the catalysts play a significant role in initiating the cracking reaction through the formation of the carbocations. However, the catalysts with high acidity tend to the formation of coke (Istadi *et al.* 2020). Therefore, the high yield of coke obtained by Ni/HY catalyst is due to the high acid site amount, especially the Lewis acid site amount. It is true since it is reported that the Lewis acid site is highly directed to the cracking reaction to produce more coke (Istadi *et al.* 2020). Interestingly, the combination of metal impregnation to HY zeolite improves the catalyst activity. As can be seen in Table 3, Ni-Co/HY catalyst has better activity than Ni/HY catalyst since the coke formation is lower than the Ni-Co/HY catalyst. The low coke formation is due to the presence of Co metal. As shown in Table 3, the Co/HY catalyst has the lowest yield of coke. Therefore, it is suggested that the Co metal leads to the lowest coke formation due to its low activity to the coke formation.

Pertaining to the selectivity of the product, as can be seen in Table 3, all catalysts have promising results as the high diversity of product distribution. However, it can be seen that the Ni-Co/HY catalyst has the highest performance in the palm oil cracking process due to its high selectivity on short-chain hydrocarbons products (gasoline). Based on Table 3, it can be seen that the product selectivity is directly proportional to the Lewis to Brønsted ratio (L/B ratio). High L/B ratio means the Lewis acid site is dominant. As can be observed, the Co/HY catalyst leads to the formation of long-chain hydrocarbons (diesel fraction) due to the low L/B ratio on the catalyst. On the other hand, the high selectivity on short-chain hydrocarbon (gasoline fraction) obtained by Ni-Co/HY catalyst is due to its high L/B ratio. Therefore, it is suggested that a low L/B ratio leads to the formation of long-chain hydrocarbon fraction. Furthermore, it is suggested that a high L/B ratio leads to the formation of short-chain hydrocarbon fraction. This finding is in accordance with Istadi *et al.* (2020). They reported that the Lewis acid site leads to the formation of short-chain hydrocarbons products in the palm oil cracking process. On the other hand, Roesyady *et al.* (2013) also reported that introducing Ni metal to the HZSM5 catalyst could increase the gasoline selectivity on palm oil cracking.

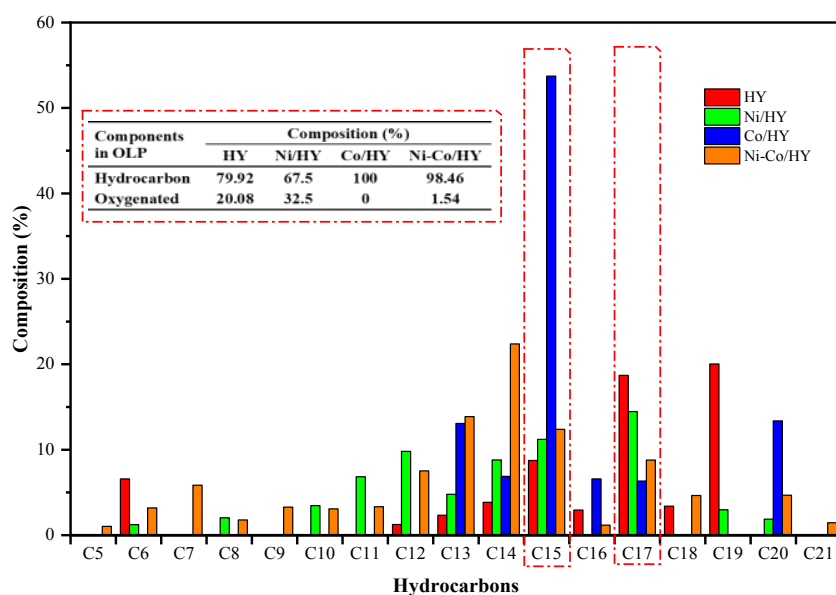


Fig. 5 Liquid products distribution and hydrocarbons distribution

Table 3 The performance of catalysts on palm oil cracking process

Parameters	Catalysts			
	HY	Ni/HY	Co/HY	Ni-Co/HY
Conversion (%)	99.04	98.52	98.79	98.66
Yield of OLP (%)	37.33	40.68	37.65	40.00
Selectivity of Gasoline (%)	6.67	9.64	0.00	11.79
Selectivity of Kerosene (%)	2.33	17.73	7.61	14.70
Selectivity of Diesel (%)	47.69	28.85	66.65	28.54
Yield of gas (%)	60.89	56.92	60.53	57.95
Yield of coke (%)	0.81	0.92	0.60	0.72

3.3 Liquid Product Distributions

The distribution of the liquid product components is also important to investigate the activity of the catalysts used. The liquid product and hydrocarbon distributions are presented in Fig. 5. As can be seen, the highest fraction of the liquid product is the hydrocarbon fraction. This result is in accordance with the study conducted by Zhao *et al.* (2015). They reported that the highest fraction in the liquid product produced from carinata oil cracking over Zn/Na-ZSM-5 catalyst was hydrocarbon. The other component is the oxygenated compounds. Based on Fig. 5, it can be observed that the highest hydrocarbon fraction is obtained by Co/HY catalyst. Therefore, it can be concluded that the Co/HY catalyst has high activity in deoxygenation reaction. It was reported in several studies that the Co metal has high activity in deoxygenation reaction (Sripta *et al.* 2015; Brillouet *et al.* 2014). On the other hand, the lowest hydrocarbon fraction is obtained by the Ni/HY catalyst. It was reported that the individual metallic Ni only catalyzed the cleavage of C–H bonds (Li *et al.* 2019). Interestingly, Ni-Co/HY catalyst also appears as an effective catalyst for the deoxygenation process since the hydrocarbon fraction obtained is high enough. Based on Table 3 and Fig. 5, it is suggested that the synergistic effect of Ni and Co impregnation on HY catalyst leads to the high selectivity in short-chain hydrocarbon fraction (gasoline ranges) and high activity in the deoxygenation process.

The high activity of Ni-Co/HY catalyst in both cracking and deoxygenation reactions is attributed to the role of each impregnated metal. The Ni metal on the catalyst has a significant role in promoting the cracking reaction, as reported in section 3.2. It has been reported that Ni-based catalysts promote the heavy hydrocarbon fractions cracking to lighter hydrocarbon fractions (Musa *et al.* 2018). On the other hand, it has also been reported that the Co-based catalysts can enhance the C(sp²)-O cleavage through direct deoxygenation pathway (Bui *et al.* 2011; Crawford *et al.* 2019). Therefore, it is suggested that the high activity of Ni-Co/HY catalyst in both cracking and deoxygenation reactions is due to the presence of Ni and Co metals.

Pertaining to the deoxygenation reaction promoted by Co/HY catalyst, it can be observed through the hydrocarbon distribution produced. In the absence of hydrogen, the deoxygenation reaction of fatty acid can be performed through decarboxylation and decarbonylation reactions. The hydrocarbons product obtained through these reactions are hydrocarbons that have one carbon shorter than the fatty acids. As the highest palm oil components are palmitic acid and oleic acid with C₁₆ and C₁₈ carbon-chains (Table 1), the hydrocarbons product produced should be C₁₅ and C₁₇ hydrocarbons. As can be seen in Fig. 5, the highest hydrocarbon fraction is C₁₅ hydrocarbon. This confirms that the Co/HY catalyst has high activity in promoting the deoxygenation reaction. On the other hand, the low enough C₁₇ fraction confirmed that the Co/HY catalyst is the potential for cracking reaction. However, its activity is still low enough. It is suggested that the C₁₇ hydrocarbons were shifted to C₁₅ hydrocarbons through β -scission of C–C bonds. As reported by Hay *et al.* (1999), the β -scission of C–C bonds of hydrocarbons components produced other hydrocarbons with two carbons shorter.

4. Conclusion

The impregnation of Ni and Co on the HY catalyst was successfully conducted. The impregnation of metal on HY catalyst increased the ratio Lewis to Brønsted acid site (L/B ratio). This ratio highly affected the cracking process of palm oil to biofuels. A high L/B ratio led to the formation of short-chain hydrocarbons, while a low L/B ratio led to the formation of long-chain hydrocarbons. The Ni impregnation on HY catalyst increased the catalyst activity in palm oil cracking. On the other hand, Co had low activity in palm oil cracking. However, Co had high activity in deoxygenation reaction. Interestingly, the co-impregnation of Ni and Co led to high activity on both cracking and deoxygenation reactions. This finding is valuable for further catalyst development, especially on bifunctional catalyst development for palm oil conversion to biofuels. However, the ratio of Ni and Co on HY zeolite has to be optimized in order to obtain the optimum catalyst activity.

Acknowledgment

The authors would like to express their sincere gratitude to the Research Institution and Community Service, Universitas Diponegoro, Semarang, Indonesia, for the financial support received under the research project of *Riset Publikasi Internasional Bereputasi Tinggi* (RPIBT) Year 2018–2020 with contract number: 387-07/UN7.P4.3/PP/2018.

References

- Adeoye, J.B., Omoleye, J.A., Ojewumi, M.E. and Babalola, R. (2017) Synthesis of Zeolite Y from Kaolin Using Novel Method of Dealumination. *International Journal of Applied Engineering Research*, 12(5), 755–760.
- Anggoro, D.D., Buchori, L., Silaen, G.C. and Utami, R.N. (2017) Preparation, characterization, and activation of Co-Mo/Y zeolite catalyst for coal tar conversion to liquid fuel. *Bulletin of Chemical Reaction Engineering & Catalysis*, 12(2), 219–226.
- Bailleul, S., Yarulina, I., Hoffman, A.E.J., Dokania, A., Abou-Hamad, E., Chowdhury, A.D., Pieters, G., Hajek, J., de Wispelaere, K., Waroquier, M., Gascon, J. and Van Speybroeck, V. (2019) A Supramolecular View on the Cooperative Role of Brønsted and Lewis Acid Sites in Zeolites for Methanol Conversion. *Journal of the American Chemical Society*, 141(37), 14823–14842.
- Bhatia, S., Mohamed, A.R. and Shah, N.A.A. (2009) Composites as cracking catalysts in the production of biofuel from palm oil: Deactivation studies. *Chemical Engineering Journal*, 155(1–2), 347–354.
- Brillouet, S., Baltag, E., Brunet, S. and Richard, F. (2014) Deoxygenation of decanoic acid and its main intermediates over unpromoted and promoted sulfided catalysts. *Applied Catalysis B: Environmental*, 148–149, 201–211.
- Buchori, L., Istadi, I., Purwanto, P. (2016) Advanced chemical reactor technologies for biodiesel production from vegetable oils - A review. *Bulletin of Chemical Reaction Engineering & Catalysis*, 11(3), 406-430.
- Bui, V.N., Laurenti, D., Delichère, P. and Geantet, C. (2011) Hydrodeoxygenation of guaiacol. Part II: Support effect for CoMoS catalysts on HDO activity and selectivity. *Applied Catalysis B: Environmental*, 101(3–4), 246–255.
- Chew, T.L. and Bhatia, S. (2008) Catalytic processes towards the production of biofuels in a palm oil and oil palm biomass-

- based biorefinery. *Bioresource Technology*, 99(17), 7911–7922.
- Corma, A. and Orchillés, A. V. (2000) Current views on the mechanism of catalytic cracking. *Microporous and Mesoporous Materials*, 35–36, 21–30.
- Crawford, J.M., Smoljan, C.S., Lucero, J. and Carreon, M.A. (2019) Deoxygenation of stearic acid over cobalt-based nax zeolite catalysts. *Catalysts*, 9(1), 42.
- Demirbas, A. (2009) Progress and recent trends in biodiesel fuels. *Energy Conversion and Management*, 50(1), 14–34.
- Feng, R., Liu, S., Bai, P., Qiao, K., Wang, Y., Al-Megren, H.A., Rood, M.J. and Yan, Z. (2014) Preparation and characterization of γ - Al_2O_3 with rich Brønsted acid sites and its application in the fluid catalytic cracking process. *Journal of Physical Chemistry C*, 118(12), 6226–6234.
- Hay, P.J., Redondo, A. and Guo, Y. (1999) Theoretical studies of pentene cracking on zeolites: C-C β -scission processes. *Catalysis Today*, 50(3–4), 517–523.
- Hewer, T.L.R., Souza, A.G.F., Roseno, K.T.C., Moreira, P.F., Bonfim, R., Alves, R.M.B. and Schmal, M. (2018) Influence of acid sites on the hydrodeoxygenation of anisole with metal supported on SBA-15 and SAPO-11. *Renewable Energy*, 119, 615–624.
- Istadi, I., Buchori, L., Anggoro, D.D., Riyanto, T., Indriana, A., Khotimah, C. and Setiawan, F.A.P. (2019) Effects of Ion Exchange Process on Catalyst Activity and Plasma-Assisted Reactor Toward Cracking of Palm Oil into Biofuels. *Bulletin of Chemical Reaction Engineering & Catalysis*, 14(2), 459–467.
- Istadi, I., Riyanto, T., Buchori, L., Anggoro, D.D., Gilbert, G., Meiranti, K.A. and Khofiyandita, E. (2020) Enhancing Brønsted and Lewis Acid Sites of the Utilized Spent RFCC Catalyst Waste for the Continuous Cracking Process of Palm Oil to Biofuels. *Industrial & Engineering Chemistry Research*, 59(20), 9459–9468.
- Kamal, P.N.S.M.M., Mohamad, N.I., Serit, M.E.A., Rahim, N.S.A., Jimat, N.I. and Alikasturi, A.S. (2020) Study on the effect of reaction and calcination temperature towards glucose hydrolysis using solid acid catalyst. *Materials Today: Proceedings*, 31, 282–286.
- Li, G., Chen, L., Fan, R., Liu, D., Chen, S., Li, X. and Chung, K.H. (2019) Catalytic deoxygenation of C_{18} fatty acid over supported metal Ni catalysts promoted by the basic sites of ZnAl_2O_4 spinel phase. *Catalysis Science and Technology*, 9(1), 213–222.
- Mhadmhan, S., Natewong, P., Prasongthum, N., Samart, C. and Reubroycharoen, P. (2018) Investigation of Ni/SiO₂ Fiber Catalysts Prepared by Different Methods on Hydrogen Production from Ethanol Steam Reforming. *Catalysts*, 8(8), 1–18.
- Musa, M.L., Mat, R. and Abdullah, T.A.T. (2018) Catalytic Conversion of Residual Palm Oil in Spent Bleaching Earth (SBE) by HZSM-5 Zeolite based-Catalysts. *Bulletin of Chemical Reaction Engineering & Catalysis*, 13(3), 456–465.
- Ramya, G., Sudhakar, R., Joice, J.A.I., Ramakrishnan, R. and Sivakumar, T. (2012) Liquid hydrocarbon fuels from jatropha oil through catalytic cracking technology using AlMCM-41/ZSM-5 composite catalysts. *Applied Catalysis A: General*, 433–434, 170–178.
- Ranga, C., Alexiadis, V.I., Lauwaert, J., Lødeng, R. and Thybaut, J.W. (2019) Effect of Co incorporation and support selection on deoxygenation selectivity and stability of (Co)Mo catalysts in anisole HDO. *Applied Catalysis A: General*, 571, 61–70.
- Riyanto, T., Istadi, I., Buchori, L., Anggoro, D.D. and Dani Nandiyanto, A.B. (2020) Plasma-Assisted Catalytic Cracking as an Advanced Process for Vegetable Oils Conversion to Biofuels: A Mini Review. *Industrial & Engineering Chemistry Research*, 59(40), 17632–17652.
- Roesyadi, A., Hariprajitno, D., Nurjannah, N. and Savitri, S.D. (2013) HZSM-5 catalyst for cracking palm oil to gasoline: A comparative study with and without impregnation. *Bulletin of Chemical Reaction Engineering & Catalysis*, 7(3), 185–190.
- Rogers, K.A. and Zheng, Y. (2016) Selective Deoxygenation of Biomass-Derived Bio-oils within Hydrogen-Modest Environments: A Review and New Insights. *ChemSusChem*, 9(14), 1750–1772.
- Sousa, F.P., Silva, L.N., de Rezende, D.B., de Oliveira, L.C.A. and Pasa, V.M.D. (2018) Simultaneous deoxygenation, cracking and isomerization of palm kernel oil and palm olein over beta zeolite to produce biogasoline, green diesel and biojet-fuel. *Fuel*, 223, 149–156.
- Sriatun, S., Susanto, H., Widayat, W. and Darmawan, A. (2019) Characteristic of ZSM-5 catalyst supported by nickel and molybdenum. *IOP Conference Series: Materials Science and Engineering*, 509, 012138.
- Srifa, A., Viriya-Empikul, N., Assabumrungrat, S. and Faungnawakij, K. (2015) Catalytic behaviors of Ni/ γ - Al_2O_3 and Co/ γ - Al_2O_3 during the hydrodeoxygenation of palm oil. *Catalysis Science and Technology*, 5(7), 3693–3705.
- Sugiarti, S., Septian, D.D., Maigita, H., Khoerunnisa, N.A., Hasanah, S., Wukirsari, T., Hanif, N. and Apriliyanto, Y.B. (2020) Investigation of H-zeolite and metal-impregnated zeolites as transformation catalysts of glucose to hydroxymethylfurfural. *AIP Conference Proceedings*, 2243, 020027.
- Vieira, S.S., Magriotis, Z.M., Ribeiro, M.F., Graça, I., Fernandes, A., Lopes, J.M.F.M., Coelho, S.M., Santos, N.A.V. and Saczk, A.A. (2015) Use of HZSM-5 modified with citric acid as acid heterogeneous catalyst for biodiesel production via esterification of oleic acid. *Microporous and Mesoporous Materials*, 201, 160–168.
- Xu, S., Zhang, Q., Feng, Z., Meng, X., Zhao, T., Li, C., Yang, C. and Shan, H. (2012) A high-surface-area silicoaluminophosphate material rich in Brønsted acid sites as a matrix in catalytic cracking. *Journal of Natural Gas Chemistry*, 21(6), 685–693.
- Yigezu, Z.D. and Muthukumar, K. (2014) Catalytic cracking of vegetable oil with metal oxides for biofuel production. *Energy Conversion and Management*, 84, 326–333.
- Zhao, X., Wei, L., Cheng, S., Cao, Y., Julson, J. and Gu, Z. (2015) Catalytic cracking of carinata oil for hydrocarbon biofuel over fresh and regenerated Zn/Na-ZSM-5. *Applied Catalysis A: General*, 507, 44–55.

